Characterization and pore structure of rice husk ash cementitious material

OJEDOKUN, Olalekan <http://orcid.org/0000-0002-9573-4976> and MANGAT, Pal <http://orcid.org/0000-0003-1736-8891>

SP-XXX—1

Characterization and Pore Structure of Rice Husk Ash Cementitious Materials

Ojedokun Olalekan and P.S. Mangat

Synopsis: An Investigation on the mineralogical and chemical characterization, pore structure, chemical shrinkage and pozzolanic activity of commercially produced rice husk ashes (RHA 1 and 2) and a control silica fume (SF) are presented in this paper. RHA possesses high silica content like silica fume which is used as supplementary cementitious materials (SCM) in the production of concrete. There is a need for an alternative to silica fume in the production of concrete because of its high demand and relatively high cost.

The mineralogical composition of RHA 1 and 2 show high silica content of 77% and 84% respectively which is close to the silica content (>80%) of class 2 silica fume. The oxides of Ca are 3.53% and 7.68% while Al is 1.19% and 1.29% for RHA 1 and 2 respectively which suggest that RHA is a low Ca^{+2} content binder. The results of chemical shrinkage of RHA 1, 2 and SF are 0.42 mL/g, 0.52 mL/g and 0.11 mL/g after 500 hrs of hydration. This indicates that RHA 2 has the highest reactivity (hydration) with water due to its highest Ca^{+2} content.

Keywords: Chemical characterization; Chemical shrinkage; Crystalline silica; Pore structure; Pozzolanic activity; Rice husk ash; Silica Fume; X-ray Diffraction and X-ray Fluorescence (XRF).

Biography: **Dr. Olalekan Ojedokun** received his PhD from Sheffield Hallam University. He is a post-doctoral researcher at the Materials and Engineering Research Institute, Sheffield Hallam University, UK and his research interest is on the utilization of rice crop waste in alkali activated cementitious materials and their durability properties.

Professor Pal Mangat is a chartered civil and structural engineer. He received his PhD degree from the University of Sheffield and was a senior lecturer in the Department of Engineering at the University of Aberdeen. He was appointed Professor of Construction Materials at Sheffield Hallam University in 1993. He has published over 100 peer reviewed publications on many novel aspects of concrete materials including accelerated curing of concrete, concrete repair and alkali activated cementitious materials.

INTRODUCTION

The need for replacing silica fume SF with rice husk ash RHA as a mineral admixture in the production of concrete arises from its high cost which is associated with the high demand of SF by many manufacturing industries in the power sector, automobile, aerospace and construction industries. On the other hand, RHA is largely disposed in landfill, which is an environmentally hazardous method of disposing waste [1]. Until recently, research efforts have been around fundamental investigations of RHA as a viable option to SF because of the high reactive silica content and the fineness of particle size in both mineral admixtures [2].

The notable improvement in the mechanical properties and durability of concrete incorporating SF is well documented in literature [3][4]. The beneficial influence of SF in concrete includes improved cohesion of the mix and reduced bleeding which enhance pumping, slipforming and finishing operation [3]. Another important property is the particle packing effect between the spaces of cement grains and at the interfacial-transition zone (ITZ) between the cement particles and aggregates. The particle packing is achieved due to the extreme fineness of silica fume particles which are 100 times smaller than the OPC particles [3]. The pore spaces in the interfacial-transition zone (ITZ) provide the weakest link in concrete, thus the particle packing effect of silica fume close to the aggregate surface improves the strength of concrete considerably [5]. The particle packing effect also improves the microstructure of SF concrete by possessing fewer pores for the ingress of deleterious substances like chloride, carbon dioxide and sulphate [4].

RHA is a natural pozzolan which is produced by burning and cooling rice husk under controlled conditions but this procedure has not been standardized. The method of burning the rice husk can result in changes to the overall mineralogical composition of the ash. It was suggested that optimum reactive RHA is produced by slow incineration of rice husk at a temperature of 500^0C to 700^0C in an industrial furnace for a few minutes until the carbon content is below 5% [6][3]. The mineralogical composition of rice husk are cellulose ($C_5H_{10}O_5$), lignin ($C_7H_{10}O_3$), hemicellulose, holocellulose and silicon dioxide [7]. These components disintegrates during the burning process leaving a high silica content in RHA similar to SF [7][6]. The pozzolanic reactivity of RHA and its potential use in the production of concrete is influenced by inherent factors such as the amorphous silica content and fineness of its grain size [8]. Preliminary research shows that a high amorphous phase of the silica content in RHA can be achieved by not exceeding 800^0C during the burning of the rice husk [7]. In addition, the reactive amorphous silica in RHA was suggested to increase by pre-treating the source material with hydrochloric acid [9]. Recent advances have been made in the pozzolanic reactivity of RHA but limited data exist in literature on the conformity criteria to achieve better durability and mechanical properties.

This paper is part of a larger research project funded by the Newton-Bhabha, UK - India programme on the utilization of the rice crop for sustainable construction/building materials which include alkali activated binders and concrete.

EXPERIMENTAL INVESTIGATION

Materials

Commercially produced RHAs investigated in this study were obtained from suppliers in India. They were supplied in 25 Kg (55.12 lb) air-tight bags. The difference in the colour of the two ashes (RHA 1 and 2) in Fig. 1 is due to the differences in the burning and cooling techniques of the rice husks to produce their ashes. A standard class 1 SF was used as the control cementitious material. It was supplied in 25 Kg (55.12 lb) drums by Elkem Materials Ltd., Sheffield, UK. SF was used to benchmark the conformity criteria of RHA for optimum durability and mechanical performance when used as a supplementary cementitious material (SCM). Ordinary Portland CEM I was used as the primary binder. It has a strength class of 52.5R and was supplied in 20 Kg (44.09 lb) bags by Frank-key Group, Sheffield, UK. CEN standard sand conforming with BS EN 1961-1 [10] was used as the fine aggregate. It was supplied by David Ball Group Ltd, Cambridge, UK. Tap water in the laboratory was used as the liquid content.

Methods

Mineralogical and Chemical Characterization

The mineralogical compositions of RHA 1, 2 and SF were analysed using a Philips X-Pert X-ray diffractometer operating with a Cu Kα radiation source (40 KV and 40 mA, wavelength λ=0.154056 nm [6.07 x10^{-9} in.]). XRD analysis of the cementitious materials (RHA 1, 2 and SF) were performed by scanning from 5^0 to 80^0 at an angle of 2Θ; the scan step size is 0.016711 and a counting time step of 0.1 s. The percentage weights of amorphous silica in RHA 1, 2 and SF were determined by the Rivetveld refinement method. This was carried out by adding a known amount of standard silicon to the cementitious material to obtain the proportion of silica in the amorphous phase.
The chemical compositions of RHA 1, 2 and SF were analysed using the wavelength dispersive Philips PW2440 sequential X-ray fluorescence spectrometer.

Chemical Shrinkage

The chemical shrinkage tests were performed on RHA 1, 2 and SF in accordance with ASTM C1608-12 [11]. The chemical shrinkage arrangement is shown in Fig. 2. RHA 1, 2 and SF pastes were produced with de-aerated water at water/cementitious ratio of 0.4. The mixing was done by hand kneading in a plastic container at 20 ±2^0C and 65% R.H. The cementitious paste was carefully placed inside glass vials to attain a paste height of 10 mm. No dispersing admixture was added during the production of the cementitious paste. The cementitious paste inside the vial was consolidated by tapping the vial on the laboratory table. The space above the cementitious paste inside the glass vial was filled with de-aerated water with the aid of a medical syringe to minimize disturbance to the surface layer of the cementitious paste. The cementitious paste was minimally dispersed during the filling but became settled 2 hrs after filling (Fig. 2). A rubber cork fitted with a capillary tube was inserted at the top of the vial containing the cementitious paste and de-aerated water. Additional de-aerated water was added via the top of the capillary tube to attain the zero-initial water height on the graduated capillary tube. Para film was wrapped around the top of the vial and rubber cork to prevent water loss. A drop of paraffin was placed inside the capillary tube to prevent evaporation. The chemical shrinkage specimens (plastic vial containing the cementitious paste) were placed inside a water bath at a temperature of 23 + 2^0C as shown in Fig. 3. The decrease in the water level was recorded for a period of 500 hrs.

Strength Activity Index (SAI)

The strength activity index (SAI) was determined in accordance with BS EN 13263-1:2005+A1:2009 [16]. A control mortar mix was produced with one-part OPC CEM 1 and three-part CEN Standard sand as specified in BS EN 196-1 [10]. The water/cement ratio was 0.5. Similar mortar mixes were produced by substituting 10% OPC CEM 1 with RHA 1, 2 and SF to produce their mortars respectively. The workability of the freshly produced mortar mixes was determined by the flow table method [17]. The mortar paste was remixed after the flow test in the Orbit mixer for 60 secs and cast into six prisms of dimensions 40 X 40 X 160 mm (1.57 X 1.57 X 6.30 in.) for each cementitious material (RHA 1, 2 and SF). The specimens in the 40 X 40 X 160 mm (1.57 X 1.57 X 6.30 in.) steel moulds were covered with polythene sheets and cured in laboratory air (22 ± 2^0C, 65 R.H.) for 24hrs. The specimens were demoulded after 24 hrs and cured in water (22 ± 2^0C) until the test ages of 7 and 28 days. Flexural and compression (equivalent cube) tests were performed on three specimens for each RHA 1, 2 and SF mortar mixes. The average strength results of the three prisms for each cementitious mortar were used to calculate the SAI at 7 and 28 days test ages. The strength activity index is the percentage strength of each cementitious mortar relative to the control OPC mortar as shown in equation 1.

$$SAI = (A/B)X100\% \quad (1)$$

Where A is the average strength of each cementitious mortar (RHA 1, 2 and SF) and B is the average strength of control OPC mortar.

Mercury Intrusion Porosimetry (MIP)

MIP samples were obtained from the inner core of RHA 1, 2 and SF mortar specimens that were used for SAI tests. The weight of the MIP samples was between 1 - 2g (0.002 - 0.004 lb) with an average length of 1 cm (0.39 in.). The MIP samples were placed in an oven (50^0C) for 3 days to remove water present within the pores of its matrix. The oven-dried samples were then placed inside a desiccator (50% R.H) for 3 days. The desiccator had silica gel at its bottom to prevent moisture migration from the air. The mercury intrusion porosimetry analyses were performed on the MIP samples using a Pascal 140/240 Porosimeter (Fig. 4). This device is in two parts; Pascal 140 which applies pressure of up to 100 MPa (14,503.8 psi) and Pascal 240 which applies pressure of up to 200 MPa (29,007.5 psi). The device measures pore sizes within the range of 0.0073 to 100 µm (2.87 x10^{-7} to 3.94 x10^{-3} in.). The computer microprocessor translates the data collected on applied pressures to pore radius using the Washburn equation (equation 2):

$$p = \frac{2\gamma \cos\phi}{\mathrm{r}} \quad (2)$$

Where $\boldsymbol{p}$ is the absolute applied pressure; $\boldsymbol{r}$ is the pore radius; $\boldsymbol{\gamma}$ is the mercury surface tension (= 0.48N/m); $\boldsymbol{\phi}$ is the contact angle (= 140^0). Washburn equation assumes that the pores in the concrete matrix are cylindrical in shape which has been criticised by many researchers. [18]

EXPERIMENTAL RESULTS AND DISCUSSION

Characterization

The chemical composition and main physical characteristics of RHA 1, 2 and SF are presented in Table 1 while the X-ray diffraction pattern is shown in Fig. 5. The three compounds responsible for the mechanical and durability properties in concrete are Si, Ca and Al. The silica content present in RHA 1 is 77% while it is 84% in RHA 2. The silica content in SF is 97% which is classified as class 1 SF [19]. However, the silica content in RHA 1 and 2 is similar to the class 2 category of SF, which is 80% as specified in BS EN 13263-1:2005+A1:2009 [19]. This suggests that RHA 1 and 2 are likely to satisfy the conformity criteria for class 2 SF based on their silica content.

The amorphous form of silica content (reactive silica) present in RHA 1, 2 and SF are 72%, 70% and 97% respectively while the corresponding total silica content is 77%, 84% and 97% respectively. This shows that despite the higher silica content of RHA 2 (84%), its reactive (amorphous) content is 70% leaving 14% unreactive silica. The corresponding values for RHA 1 are total silica content of 77%, reactive (amorphous) silica 70% leaving 5% unreactive silica. SF is 97% amorphous silica. RHA 1 shows a lower risk of health hazard (silicosis) associated with high content of crystalline silica when used as cementitious material. No crystalline silica (unreactive silica) is present in SF sample. The unreactive silica content of RHA is within the limits provided in materials safety data sheet (MSDS).

The calcium content present in RHA 1, 2 and SF samples are 3.53%, 7.68% and 0.27% respectively (Table 1) while the alumina contents are 1.19%, 1.29% and 0.57% respectively. RHA 2 possesses higher Ca and Al content than RHA 1 which might result in better pozzolanic and mechanical strength properties.

The mineralogical compositions in the X-ray diffraction pattern of RHA 1 (Fig 5a) show peaks for Quartz and Cristobalite polymorphs of SiO_2, as well as silicon. XRD on RHA 2 sample shows peaks for Quartz and Calcite ($CaCO_3$), as well as silicon. XRD on SF sample only shows peaks for silicon, the sample is completely amorphous. The peaks of Quartz and Cristobalite polymorphs of SiO_2 are present in the RHA samples presented by Ayomanor and Vernon-parry [20]. These peaks are the crystalline phase of the silica content which is attributed to the high temperature of the burning process of RHA. The optimum burning temperature of 500^0C to 700^0C [6][3] that should sustain the amorphous phase of the RHA may have been exceeded in both RHA 1 and 2.

Alkalinity

The pH of RHA 1, 2 and SF are 9.87, 10.84, and 8.72 respectively as shown in Table 1. The pH of the cementitious material is influenced by the Ca^{+2} content. The Na^+ and K^+ content also contribute to the alkalinity of the cementitious materials. RHA is likely to consume lesser $Ca(OH)_2$ than SF during the secondary pozzolanic reaction with the hydration product of OPC cement. The reduction of free lime, $Ca(OH)_2$, induced by the secondary pozzolanic reaction can promote a faster rate of carbonation [21][22][23] and corrosion in supplementary cementitious materials SCM concrete compared with OPC concrete. The high alkalinity of RHA 1 (9.87) and 2 (10.84) compared with SF (8.72) may result in better durability properties of concrete when prepared with RHA.

Chemical Shrinkage

The chemical shrinkage of RHA 1, 2 and SF after 500 hrs hydration time is shown in Fig. 6. The chemical shrinkage of RHA 1 and 2 are considerably higher than silica fume. The cementitious materials (RHA 1, 2 and SF) were activated with water to estimate their reactivity relative to SF although it is recognised that water is not the ideal medium for hydration of these pozzolanic materials. The results of chemical shrinkage of RHA 1, 2 and SF are 0.42 mL/g, 0.52 mL/g and 0.11 mL/g after 500 hrs of hydration. This suggests that RHA 2 is more reactive with water than RHA 1 and SF because of the highest Ca^{+2} content of 7.67% present in RHA 2 (Table 1) which may be responsible for the faster rate of hydration. The Ca^{+2} content in RHA 1 and SF are 3.53% and 0.27% respectively. The considerably low chemical shrinkage of SF (0.11 mL/g) after 500 hrs of hydration could be because of the low Ca^{+2} content of 0.27% (Table 1).

Chemical Shrinkage Model

Studies on the prediction of ultimate volume based on the hydration stoichiometry of Portland cement (PC) shows realistic results [13][14]. However, De Belie *et al*. [15] pointed out the difficulty of relating chemical shrinkage to the degree of reactions for supplementary cementitious materials (SCM) because the exact stoichiometry of SCM and their specific volumes are not well established. The authors' [15] argument is based on the invalid assumption of selective dissolution of anhydrous Portland cement occurring before the dissolution of supplementary cementitious materials. The hydration model presented by Bentz *et al.* [12] for pozzolanic materials is adopted in this study. The ultimate volume change of the chemical reactants is determined from the hydration reaction of pozzolanic materials, specific gravity and their molar volumes. The hydration stoichiometry of silica (pozzolanic reaction) is given equation 1.

Silica (pozzolanic reaction) $1.1\ CH + S + 2.8\ H \longrightarrow C_{1.1}SH_{3.9}$ (1)

Where CH is calcium hydroxide, S is silicate, H is water and CSH is the calcium silicate hydrate.
The ultimate volume is calculated from the differences in volume between the basic reactant and the final hydration product. The ultimate volume is calculated from molar weight and specific gravity of each molecular component as described in the following equations:

	1.1 CH	+	S	+	2.8 H	=	$C_{1.1}SH_{3.9}$
Molar weight (g/mole)	81.4		28.09		50.44		203.15
Specific gravity (g/cm^2)	2.21		2.33		1.0		2.12
Molar Volume (cm^2/mole)	36.83		12.05		50.44		95.83
Ultimate Volume (cm^2)	= (36.83 + 12.05 + 50.44) - 95.83 = 3.49 cm^2 (0.54 in^2)						
Chemical Shrinkage (mL/g)	3.49/28.09		=		0.124mL/g of hydrated silicate		

The chemical shrinkage of silicate hydrate from the hydration stoichiometry of silica (pozzolanic reaction) from equation 1 using the molar weight and specific gravity shows a good prediction relative to experimental data for silica fume (Fig. 6). The prediction is valid for RHA 1 and 2 for 24 hrs hydration only. The chemical shrinkage in RHA 1 and 2 is significantly higher after 24 hrs hydration. This suggests that the hydration stoichiometry of silica (pozzolanic reaction) from equation 1 cannot be used universally for all pozolanic materials confirming the conclusion made by De Belie *et al*. [15]. This is also due to the much higher amount of CaO in RHA 1 and 2.

Strength Activity Index

The strength activity index SAI of RHA 1, 2 and SF is shown in Fig. 7. SF shows considerably higher SAI than RHA 1 and 2. The SAI for RHA 1, 2 and SF at 7 days is 75%, 81% and 110% respectively while it is 89%, 93% and 123% at 28 days. The high reactive silica content in SF of 97.18% aided the superior strength property compared with RHA 1 and 2 which had 72% and 70.13% of reactive silica content respectively. The other important factor affecting strength performance of concrete is their fineness. RHA 1 and 2 were used in making their respective mortars as received from the suppliers in India. On the other hand, the particle size of SF is finer than RHA 1 and 2. SF has less than 10% retained on 45 µm (1.77 X 10^{-3} in.) sieve and specific surface area, SSA, of 20,000 m^2/Kg (97,649 ft^2/lb) [24]. *Antiohos et al.* [8] suggested that 10% replacement in concrete with RHA ground in the laboratory to a SSA of 7,000 m^2/Kg (34,177 ft^2/lb) exhibited similar strength to the reference OPC concrete. The particle size of RHA that has specific surface area of 7,000 m^2/Kg (34,177 ft^2/lb) will have more than 10% retained on 45 µm (1.77 X 10^{-3} in.) sieve unlike SF with SSA of 20,000 m^2/Kg (97,649 ft^2/lb). The strength performance of RHA in concrete is subject to the fineness of its particle sizes [25][26]. The fineness of RHA 1, 2 and SF will be carried out in subsequent test to quantify its influence on the strength performance.

Pore Structure

The pore size distribution and effective porosity of OPC, RHA 1, 2 and SF mortars are shown in Figures 8 and 9 respectively. The pore size distribution of OPC, RHA 1, 2 and SF mortars at 28 days age in Fig. 8 shows similar single range of pore volume within the differential pore distribution graph (i.e. unimodal pore distribution) which has high volume of its pore diameters within 0.05 µm and 0.2µm (1.97 x10^{-6} to 7.87 x10^{-6} in.), however, the differential pore volume differs. The peak differential pore volumes within 0.05 µm and 0.2µm (1.97 x10^{-6} to 7.87 x10^{-6} in.) pore diameters are 77 m^2/g (375,947 ft^2/lb), 73 m^2/g (356,417 ft^2/lb), 96 m^2/g (468,713 ft^2/lb) and 44 m^2/g (214,827 ft^2/lb) for OPC, RHA 1, 2 and SF mortars respectively. SF mortar has the lowest differential pore volumes unlike the RHA mortars which show considerably higher differential pore volumes within the same pore diameter. The pore/solid ratio of SF mortar will be lower due to lesser pore volume than RHA. This explains the superior strength performance of SF mortar than RHA mortar as shown in Fig. 7.

The effective porosity of OPC, RHA 1, 2 and SF mortars at 28 days age are 8.9%, 9.17%, 10.4% and 8.19% respectively as shown in Fig. 9. The result of the effective porosity complements the lowest differential pore volume of SF (Fig. 8) and the highest strength activity index SAI (Fig. 7) compared to RHA mortar which had higher differential pore volume and a lower SAI at 28 days age. The pore filling effect of SF in mortars is more pronounced than RHA.

Strength - Porosity Relationship

The relationship between strength and porosity of the supplementary cementitious mortars at 28 days age is shown in Fig. 10. A non-linear equation between porosity and strength is provided by the regression analysis of the data in Fig. 10, which gives:

$$\sigma = 959.34\,(1-p)^{-1.29} \quad (2)$$

Where σ is the compressive strength; p is volume of voids expressed as a fraction of the total volume of mortar, with a coefficient of correlation of 0.80.

The graph shows a non-linear relationship similar to the model proposed by *Balshin* [27], with the lowest porosity producing highest strength. The densification of microstructure due to the filler effect of the extremely fine SF and its highest reactive silica content of 97% produced the highest strength. RHA mortar has higher porosity and lower strength as a result of the lower specific surface area reflecting in its larger grain sizes than SF mortar.

CONCLUSIONS

Commercially produced rice husk ashes (RHA 1 and 2) and a control sample of silica fume (SF) were investigated to determine the mineralogical composition by X-ray Diffraction (XRD) analysis, the chemical composition by X-ray Fluorescence (XRF) analysis, pore structure by mercury intrusion porosimetry (MIP), chemical shrinkage and the strength activity index. The following conclusions are drawn based on the results of this experimental investigation:

1. The two RHA ashes have high silica content similar to class 2 SF while the calcium and alumina content is higher than SF. The total silica content of the two rice husk ashes is 77% and 84% and the corresponding reactive (amorphous) silica content is 72% and 70%. The crystalline silica content of the RHAs is 5% and 14% respectively which is within the safe limit provided in materials safety and data sheets. The silica, CaO and Al_2O_3 contents are the primary constituents of RHA ashes that aid concrete properties.
2. Chemical shrinkage tests reveal that RHA is more reactive in hydration with water than SF due to its higher calcium content. The higher calcium content equally contributes to the higher pH of the RHA.
3. The strength activity index, SAI, of RHA mortar is lower than SF (class 1) mortar. The SAI are 75%, 81% and 110% for RHA 1, 2 and SF at 7 days while it is 89%, 93% and 123% at 28 days respectively.
4. The strength-porosity relationship of RHA and SF mortars conforms to relationships proposed for porous materials, which is in the form: $\sigma = \sigma_0\,(1-p)^n$ with correlation of 0.8.
   Where σ is the compressive strength; σ_0 is the compressive strength of fully dense material; p is volume of voids expressed as a fraction of the total volume of mortar; n is a constant.

ACKNOWLEDGMENTS

The authors gratefully acknowledge the funding provided by the UK - India Governments' Newton - Bhabha research programme. The funding was provided through Department of Biotechnology, Innovate UK, EPSRC for research on Valorisation of Rice Milling by-products by their utilisation in cementitious materials. They also acknowledge the continuing support of the Materials and Engineering Research Institute, Sheffield Hallam University.

REFERENCES

[1] A. P. Gidde, M.R., Jivani, "Waste to Wealth - Potential of Rice Husk in India a Literature Review," *Proc. Int. Conf. Clean. Technol. Environ. Manag.*, pp. 586–590, 2007.

[2] P. K. Mehtra and K. J. Folliard, "Rice Husk Ash--a Unique Supplementary Cementing Material: Durability Aspects," *Spec. Publ.*, vol. 154, pp. 531–542, May 1995.

[3] A. M. Neville, *Properties of Concrete*, vol. Fifth. Pearson Education Limited, 2011.

[4] P. S. Mangat and B. T. Molloy, "Influence of PFA, slag and microsilica on chloride induced corrosion of reinforcement in concrete," *Cem. Concr. Res.*, vol. 21, no. 5, pp. 819–834, 1991.

[5] J. A. Larbi, "Microstructure of the interfacial zone around aggregate particles in concrete," *Heron*, vol. 39, no. 1, pp. 1–69, 1993.

[6] Min-Hong Zhang and V. Mohan Malhotra, "High-Performance Concrete Incorporating Rice Husk Ash

as a Supplementary Cementing Material," Title nos. 93-M72, 1996.
[7] S. Kumar, P. Sangwan, D. R. M. V, and S. Bidra, "Utilization of Rice Husk and Their Ash : A Review," *J. Chem. Environ. Sci.*, vol. 1, no. 5, pp. 126–129, 2013.
[8] S. K. Antiohos, V. G. Papadakis, and S. Tsimas, "Rice husk ash (RHA) effectiveness in cement and concrete as a function of reactive silica and fineness," *Cem. Concr. Res.*, vol. 61–62, pp. 20–27, 2014.
[9] Q. Feng, H. Yamamichi, M. Shoya, and S. Sugita, "Study on the pozzolanic properties of rice husk ash by hydrochloric acid pretreatment," *Cem. Concr. Res.*, vol. 34, no. 3, pp. 521–526, 2004.
[10] B. Standards, "BS EN 196-1: Methods of testing cement — determination of strength," 2005.
[11] ASTM Committee C01.31, "ASTM C1608-12 Standard Test Method for Chemical Shrinkage of Hydraulic Cement Paste," in *Annual Book of ASTM Standards Volume 04.01*, 2012, pp. 1–5.
[12] D. P. P. Bentz, O. M. Jensen, a. M. Coats, and F. P. P. Glasser, "Influence of silica fume on diffusivity in cement-based materials I. Experimental and computer modeling studies on cement pastes," *Cem. Concr. Res.*, vol. 30, no. 6, pp. 953–962, 2000.
[13] E. E. Holt, "Early age autogenous shrinkage of concrete," *VTT Publ.*, no. 446, pp. 2–184, 2001.
[14] E. ichi Tazawa, S. Miyazawa, and T. Kasai, "Chemical shrinkage and autogenous shrinkage of hydrating cement paste," *Cem. Concr. Res.*, vol. 25, no. 2, pp. 288–292, 1995.
[15] N. De Belie *et al.*, "Determination of the degree of reaction of fly ash in blended cement pastes," *14th Int. Congr. Chem. Cem. Proc.*, pp. 1–12, 2015.
[16] BS EN 13263-1:2005+A1:2009, *Silica fume for concrete. Definitions, requirements and conformity criteria*. British Standards.
[17] BS EN 413-2:2016, *Masonry cement. Test methods*. .
[18] N. Hearn and R. D. Hooton, "Sample mass and dimension effects on mercury intrusion porosimetry results," *Cem. Concr. Res.*, vol. 22, no. 5, pp. 970–980, 1992.
[19] BS EN 13263-1:2005+A1:2009, *Silica fume for concrete. Definitions, requirements and conformity criteria*. British Standards.
[20] B. O. Ayomanor and K. Vernon-parry, "Potential Synthesis of Solar-Grade Silicon from Rice Husk Ash," *Solid State Phenom.*, vol. 242, pp. 41–47, 2016.
[21] D. W. S. Ho and R. K. Lewis, "Carbonation of concrete and its prediction," *Cem. Concr. Res.*, 1987.
[22] M. I. Khan and C. J. Lynsdale, "Strength, permeability, and carbonation of high-performance concrete," *Cem. Concr. Res.*, 2002.
[23] E. Gruyaert, P. Van Den Heede, and N. De Belie, "Carbonation of slag concrete: Effect of the cement replacement level and curing on the carbonation coefficient - Effect of carbonation on the pore structure," *Cem. Concr. Compos.*, 2013.
[24] Elkem Microsilica Concrete, "Guidance for the Specification of Silica Fume."
[25] A. N. Givi, S. A. Rashid, F. N. A. Aziz, and M. A. M. Salleh, "Assessment of the effects of rice husk ash particle size on strength, water permeability and workability of binary blended concrete," *Constr. Build. Mater.*, vol. 24, no. 11, pp. 2145–2150, 2010.
[26] M. H. Zhang, R. Lastra, and V. M. Malhotra, "Rice-husk ash paste and concrete: Some aspects of hydration and the microstructure of the interfacial zone between the aggregate and paste," *Cem. Concr. Res.*, vol. 26, no. 6, pp. 963–977, 1996.
[27] Balshin M.Y., "Relation of Mechanical Properties of Powder Metals and their Porosity and the Ultimate Properties of Porous-Metal Ceramic Materials," vol. 67, no. 5, pp. 831–834, 1949.

TABLE AND FIGURES

Table 1–Chemical composition and main physical characteristics of RHA 1, 2 and SF

	RHA 1	RHA 2	SF
Na_2O, %	-	0.62	-
MgO, %	0.41	1.13	0.23
Al_2O_3, %	1.19	1.29	0.57
SiO_2, %	77.00	84.13	97.18
SiO_2 (reactive), %	72.00	70.13	97.18
P_2O_5, %	2.38	1.43	0.64
SO_3, %	0.88	0.28	0.14
K_2O, %	9.85	2.07	0.82
CaO, %	3.53	7.68	0.27
TiO_2, %	0.37	0.05	-
MnO, %	0.40	0.08	-
Fe_2O_3, %	2.24	0.89	0.12
ZnO, %	-	0.02	0.03

SrO, %	-	0.02	-
BaO, %	-	0.10	-
Cl, %	1.77	0.24	0.30
LOI, %	14.30	4.8	6.0%
Specific surface area			13.5m^2/g
pH	9.87	10.84	8.72

1

Fig. 1–Samples of cementitious materials RHA 1, 2 and SF in self-sealing bags

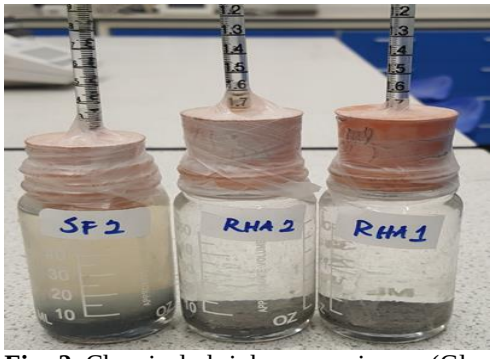

Fig. 2–Chemical shrinkage specimens (Glass vials with paste) of RHA 1, 2and SF

2

Fig. 3 – Chemical shrinkage specimens in water bath (23 + 2^{0}C)

Fig. 4 – Mercury intrusion porosimetry (MIP) device

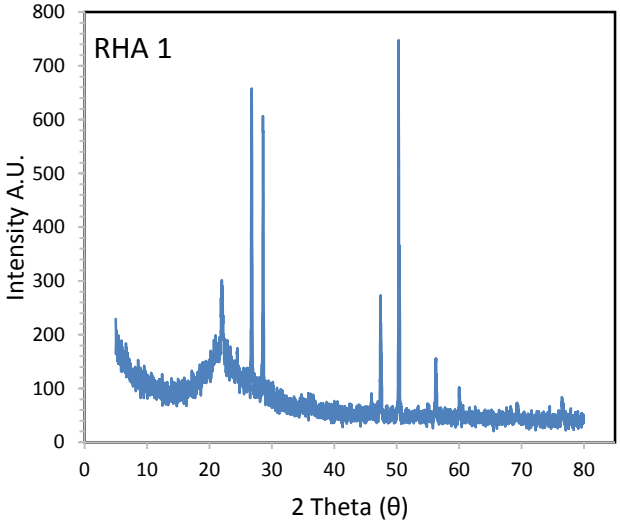

(a)

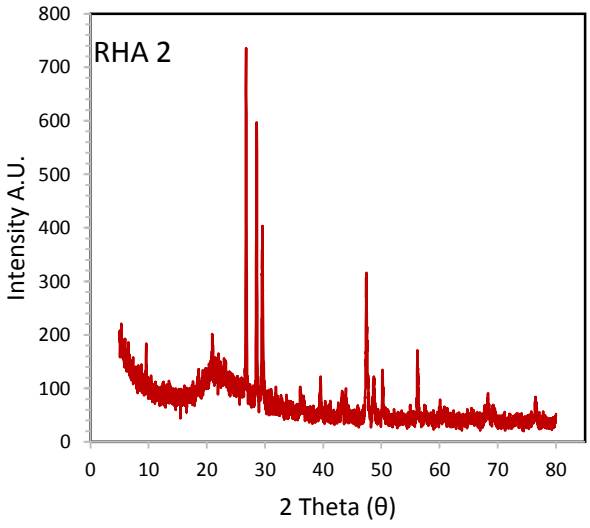

(b)

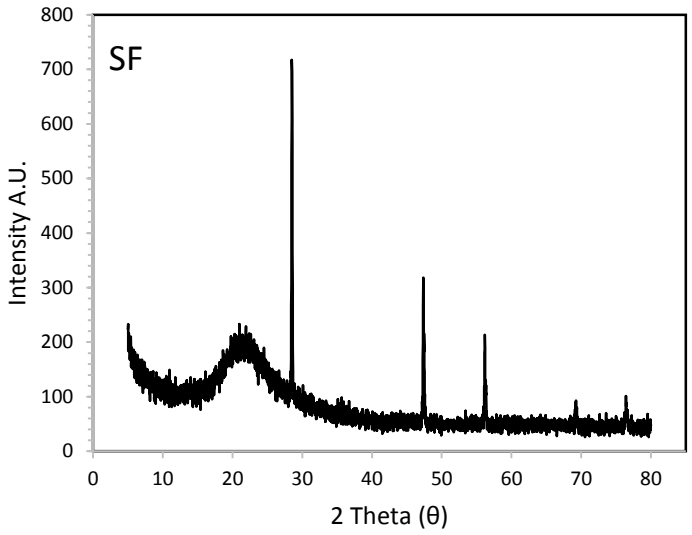

(c)

Fig. 5 – X-ray diffraction patterns of (a) RHA 1 (b) RHA 2 and (c) SF

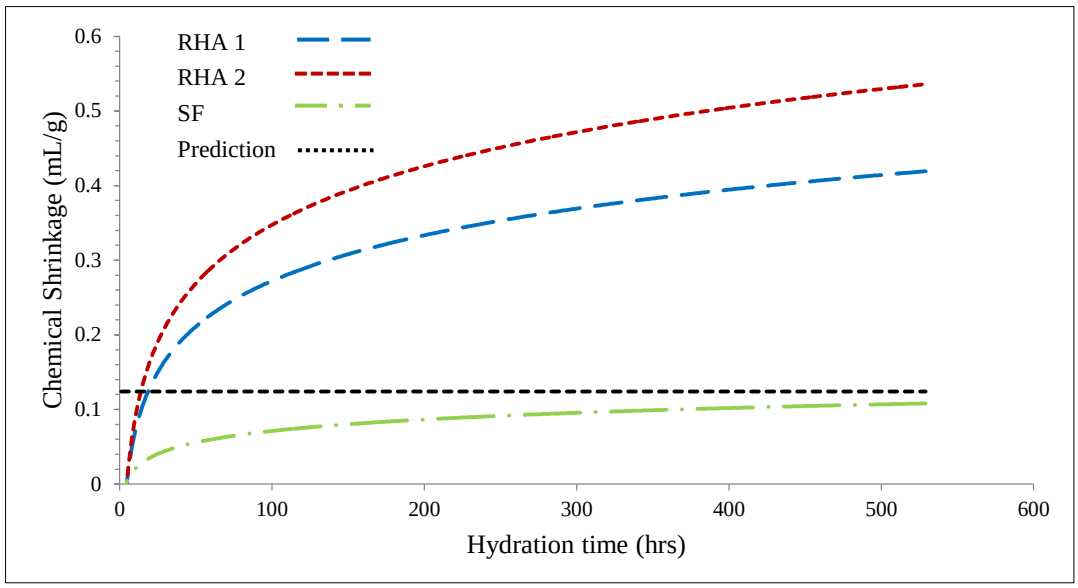

Fig. 6 – Chemical shrinkage of RHA 1, 2 and SF after 500 hrs hydration time

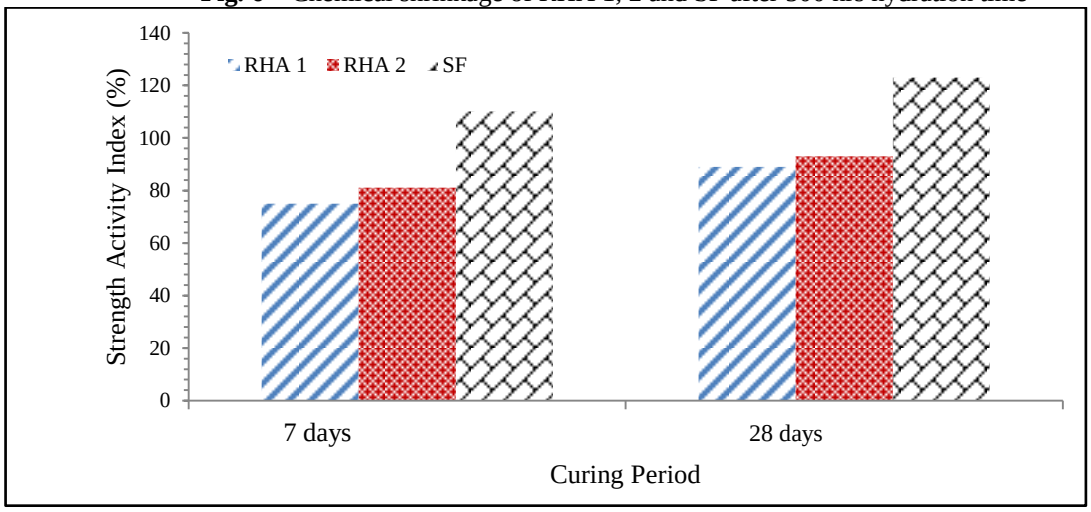

Fig. 7 – Strength activity index of RHA 1, 2 and SF at 7 and 28 days

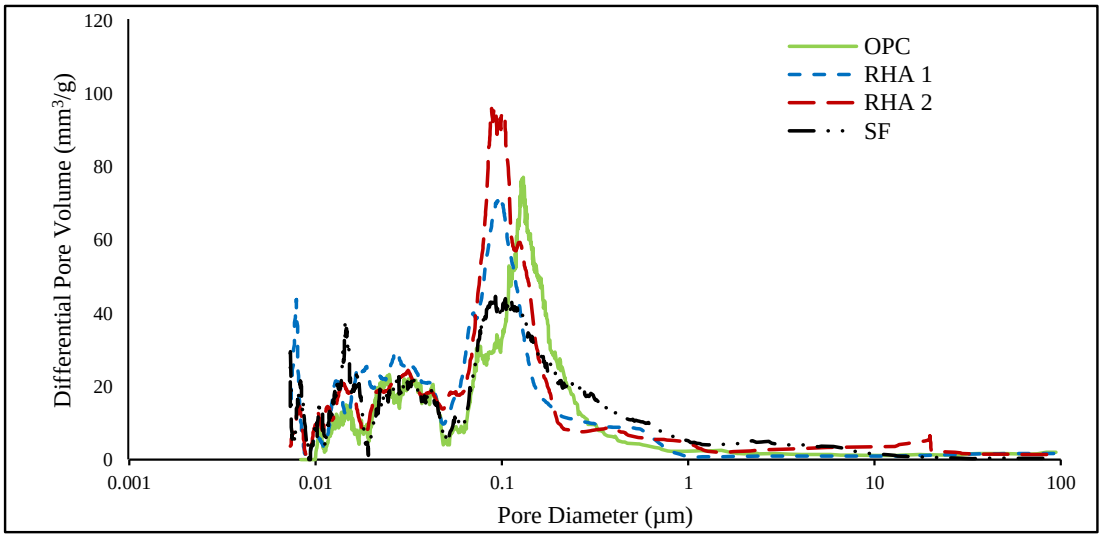

Fig. 8 – The pore size distribution of OPC, RHA 1, 2 and SF mortars at 28 days age

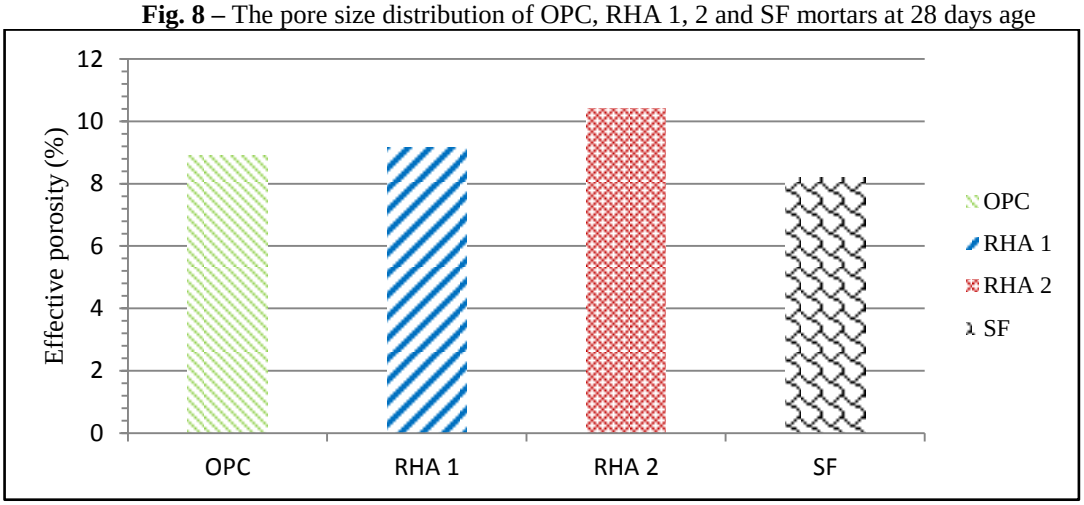

Fig. 9 – The effective porosity of OPC, RHA 1, 2 and SF mortars at 28 days age

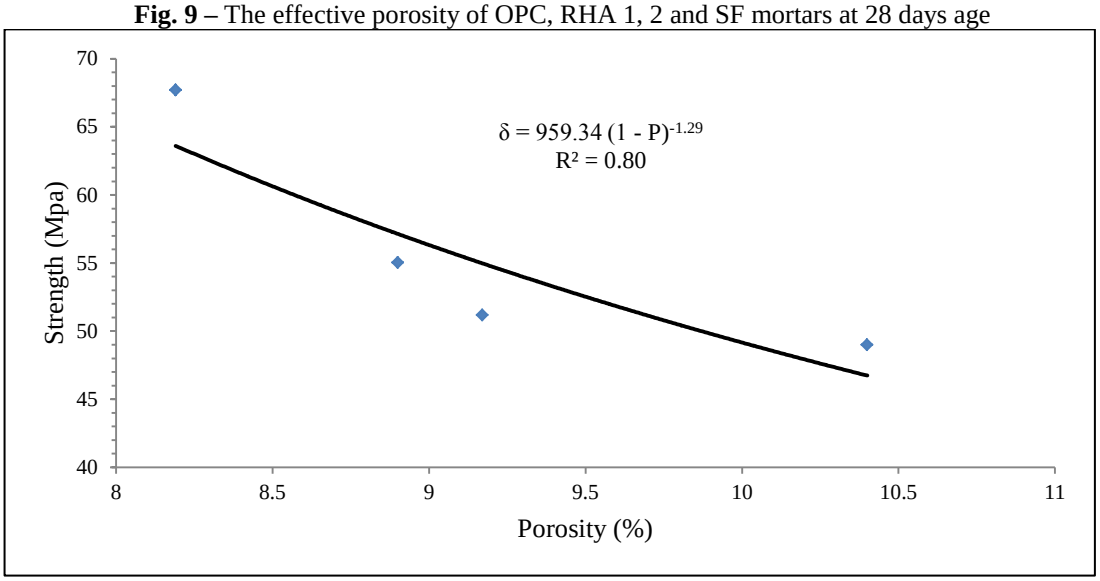

Fig. 10 – Strength-porosity relationship of OPC, RHA and SF mortars